

High Performance Dual Polarized Near-Field Probe at V-Band Provides Increased Performances for Millimeter Wave Spherical Near-Field Measurements

A. Giacomini, L. J. Foged
Microwave Vision Italy s.r.l.
Via dei Castelli Romani, 59
00071 Pomezia, Italy
andrea.giacomini@microwavevision.com

E. Szpindor, W. Zhang, P. O. Iversen
Orbit/FR Inc.
650 Louis Dr., Suite 100
Warminster, 18974, PA, USA
peri@orbitfr.com

Abstract— V-band (50-75GHz) applications such as 5G and myriad others are the catalyst for high performance near-field antenna measurement systems. For Spherical Near-Field (SNF), the traditional approaches at millimeter wave frequencies collect two full spheres of data in the near-field where each sphere samples one of two linear and orthogonal fields of the antenna under test (AUT). These two orthogonal polarizations are traditionally achieved through mechanical rotation of a single polarized probe. To improve measurement time and accuracy, MVG has developed a dual polarized V-band probe. This probe has been integrated in a millimeter wave SNF system (μ -Lab) and is connected to two simultaneously sampled parallel receiver channels. This approach only requires one sphere to be measured and it ensures the two polarization components are sampled at the same point in space and time. The SNF probe design proposed in this paper is based on an axially corrugated aperture. The probe includes a compact integrated OMT and the ports are WR-15 waveguide. This paper will present the design requirement, design details, and measured performances of the proposed dual polarized SNF probe.

I. INTRODUCTION

The expanding market for millimeter wave antennas is driving the need for high performance near-field antenna measurement systems at these frequencies. Traditionally, at millimeter waves, acquisition of two orthogonal polarizations have been achieved through mechanical rotation of a single polarized probe and an associated frequency conversion modules. This generally results in the collection of two complete spherical data sets, one for each polarization, significantly separated in time.

To enable improvements in both measurement speed and accuracy, MVG has developed a new high performance dual polarized feed in V-band (50-75GHz). This probe has been integrated in a millimeter wave Spherical Near-Field (SNF) system (μ -Lab) [1]-[5] via two parallel receiver channels that are simultaneously sampled. The facility [6] is shown in Figure 1. This architecture more than doubles the acquisition speed and additionally ensures that the two polarization components are sampled at precisely the same point in space and time. This is beneficial when polarization analysis is required from the

acquired data set, e.g. conversion of dual linear polarization to spherical/elliptical polarizations.



Figure 1. : MVG μ -Lab: millimeter wave Spherical Near-Field measurement system.

The SNF probe design proposed in this paper is based on an axially corrugated aperture providing medium gain radiation patterns. The directivity versus beam-width of the aperture has been tailored to the measurement system, ensuring proper AUT illumination and sufficient gain to compensate for free space path loss. Dual polarization capability is achieved with an integrated OMT feeding directly into the probe circular waveguide. Thanks to the balanced feeding used for each polarization, the port-to-port coupling is sufficiently low to allow for simultaneous acquisition of the two channels. Input ports are WR-15 waveguide interfaces to simplify the integration with the system front-end.

This paper will present the detailed description and measured performances of the proposed dual polarized SNF probe. The organization of this paper is as follows: Section II describes the upgrade of the RF architecture of the MVG millimeter wave SNF system (μ -Lab) and the need of a dedicate probe design; Section III describes the main requirements and design drivers for the probe development; Section IV deals with the probe design and trade-off considerations; Section V illustrates the probe characterization through conducted and radiated measurements.

II. RF ARCHITECTURE UPGRADE OF μ -LAB

The main motivation behind the upgrade of the existing μ -Lab system is a reduction of the measurement time with the use of two simultaneous receiver channels. This allows dividing the measurement time by a factor of two compared to the traditional architecture. As an example, with the current hardware, the typical measurement duration at V-band of an AUT with 8cm radiating aperture, requiring a 2.5° sampling, is approx. 1.5 hours. This time includes the acquisition of the two full spheres in approx. 101 frequency points.

At millimeter waves, and more in general above 50GHz, the increase of measurement speed by switching different channels of a dual polarized probe cannot be accomplished as commonly done at lower frequency bands. PIN diode devices cannot be found yet on the market with reasonable isolation and insertion loss figures.

Alternately, electro-mechanical techniques are usually considered by rotating the single polarized probe using motors and solenoids. The main drawback is that any RF moving part has a negative impact on the system durability and the polarization accuracy. As an example, a phase drift due to measurement duration (over 1 hour) and moving RF cables can easily reach 5-7° in practical situations. Such a phase error would give approx. 1dB axial ratio when deriving circular polarization from two linear components. In some specific cases, when measurement time is extended (i.e. multi-beam arrays with hundreds/thousands of states) or AUT characteristics may change quickly, the system stability has a crucial impact.

The use of a hardware configuration with two simultaneous receiver channels connected to a static dual polarized probe is therefore the preferable solution. The actual configuration of the μ -Lab requires an upgrade of the RF architecture and the development of a dedicate dual polarized probe suited for SNF applications.

The current system configuration based on the use of a single polarized probe is depicted in Figure 2. The VNA is used as a source and receiver, providing two coherent local oscillator (LO) sources. The probe is rotated with a polarization positioner, either manually or automated, to acquire the H- and V-polarization components. A single millimeter wave frequency down converter is used in the receiver path to down convert the measured signal to intermediate frequency (IF).

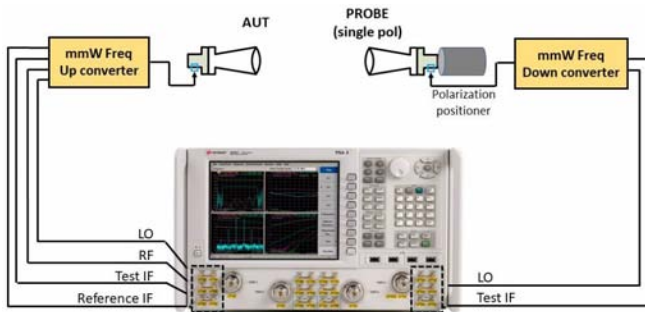


Figure 2. : RF architecture with a single polarized probe and mechanical polarization positioner.

Upgrading the configuration to dual polarization requires two millimeter wave frequency down converters connected to the probe ports. The received signals for H- and V-polarizations are simultaneously down converted and the associated IF channels are measured by the VNA. The block diagram of this configuration is represented Figure 3.

The two measurement channels are calibrated via radiated boresight measurements over a range of polarization angles, generating a four term “ortho-mode” correction matrix vs. frequency.

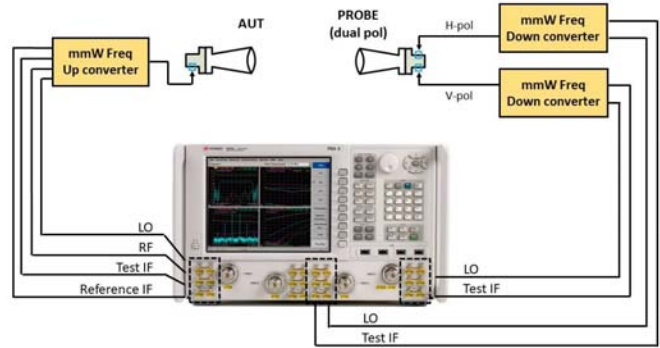


Figure 3. : RF architecture with a dual polarized probe and two simultaneous receiver channels.

III. PROBE REQUIREMENTS

The requirements considered for the probe development are those typical of spherical near field measurement applications [7]-[9]. Besides bandwidth and dual polarization capabilities, which are convenient features for time-efficient testing [10], the principal design trade-off is about directivity versus and pattern beam-width. The geometrical characteristics of the facility, such as test distance and maximum AUT size, allow to define quantitative requirements on these parameters. At millimeter wave, the over-the-air attenuation of the test scenario is usually significant and it is highly desirable to compensate it with higher gain probes, to ensure reasonable dynamic range to the measurement. On the contrary, the AUT illumination should be sufficiently uniform in amplitude and phase taper at the edge of the test zone, in order to maintain good accuracy even if NF-FF transformation is calculated without probe correction. In the case that the AUT becomes large with respect to the test distance, then probe correction becomes necessary and an additional probe characteristic comes in the list of requirements. In this case, the probe should be a good approximation of a first order probe ($|M|=1$) in terms of spherical mode content, avoiding more complex full probe correction techniques [11]-[12].

Since the facility upgrade is based on a parallel receiver architecture to increase measurement speed, the probe ports should have sufficient port-to-port isolation to allow for simultaneous sampling acquisition. Cross-polarization discrimination is also a relevant figure of merit for the application, with the on-axis performance being the most relevant feature. In regards to the mechanical characteristics, the probe envelope should be minimized in order to preserve the AUT-probe distance. The probe should be equipped with

absorbing provisions and with a precision interface for accurate positioning and alignment, critical aspects at millimeter waves. The probe should have waveguide input ports for easy mating with the RF front-end, based on WR-15 waveguide standard. Table I. highlights the probe requirements based on the considerations above and defines numerical figures.

TABLE I. PROBE SPECIFICATIONS

Item	Specification	Comments
Frequency	50 – 75GHz	V-band
Waveguide standard	WR-15	nominal band: 50-75GHz cut-off @ 39.9GHz overmoding @ 79.7GHz
RF flange	UG385/U	w/o anti-cocking
Polarization	Dual	H/V
Directivity	14dBi	trade-off between path loss and edge taper
HPBW	> 30°	double-sided, equal in E- and H-planes
Cross-polar discrimination	> 40dB	on-axis, often additional value specified at probe field-of-view
Pattern shape	M ~ +/-1	for first order probe correction (if needed)
Return loss	> 10dB	not critical at system level
Isolation	> 40dB	for simultaneous acquisition
Physical envelope	minimum length	absorber screen to be integrated

IV. PROBE DESIGN

The probe design is based on a medium gain (~13dBi) radiating aperture with multiple axial corrugations [13]-[14], providing symmetric pattern cuts and low cross-polarization levels in the diagonal planes. The directivity versus beam-width has been tailored to the measurement system layout, providing equalized pattern cuts with approx. 35° double-sided HPBW over the frequency range. This value ensures proper AUT illumination and sufficient gain to compensate for free space path loss in the set-up. Dual polarization capability is achieved with an integrated turnstile OMJ [15]-[16] feeding directly into the probe circular waveguide. Matching is improved by a conical matching stub at the bottom of the feeding cavity. Details of the feeding section are shown in the cross-section of the structure presented in Figure 4. Thanks to the balanced feed used for each polarization, the port-to-port isolation is sufficiently low to allow for simultaneous acquisition of the two linear field components. Input ports are

standard WR-15 waveguide to simplify the integration with the front-end.

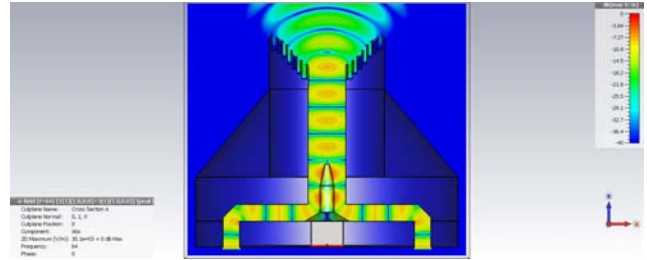


Figure 4. : Details of the probe feeding structure with simulated E-field @ center frequency.

The probe geometrical layout is depicted in Figure 5. , as taken from the CAD electrical model. This figure shows the different components: the corrugated radiating aperture, the OMJ and the X and Y feeding networks with their physical offset along the probe axis. It should be noted that, in the modeling, the absorptive backing screen is replaced by a fully metallic skirt to avoid unnecessary complexity the absorbing material would introduced in the computation.

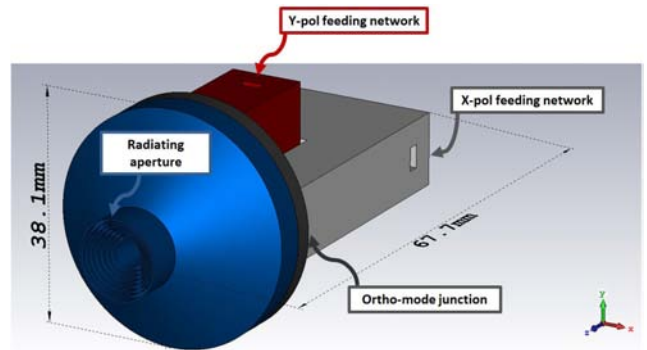


Figure 5. : CAD model and port definition.

The simulated results reported in the following are obtained from high fidelity time-domain modeling [17]. The S-parameters at the input ports of the probe assembly calculated over an extended frequency band are reported in Figure 6. The curves are referenced to the WR-15 waveguide standard, with inner dimensions of 0.148’’x0.074’’ [18]. The reflection coefficients are below -10dB over the entire nominal band, while the port-to-port isolation shows excellent theoretical performance, with sufficient design margin.

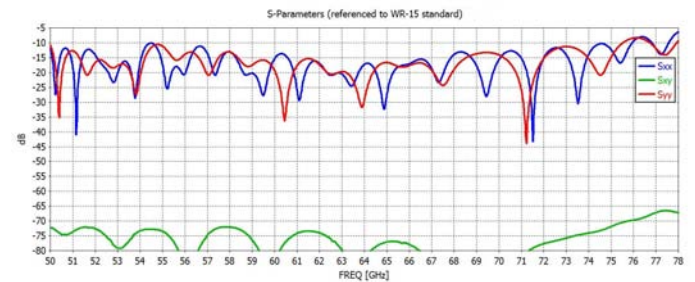


Figure 6. : S-parameters referenced to WR-15 standard.

Boresight directivity and half power beam-width (double-sided), reported in Figure 7. and Figure 8. , show that the AUT illumination is within the defined requirements and is almost frequency independent.

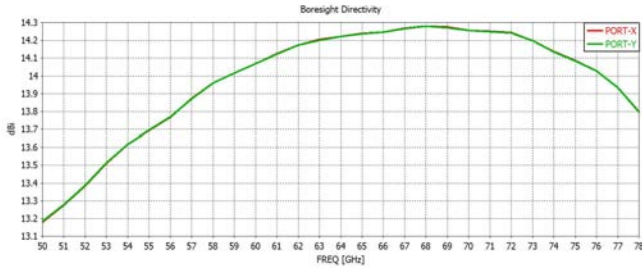


Figure 7. : Simulated boresight directivity.

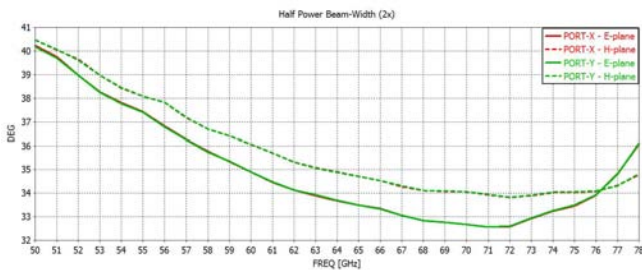


Figure 8. : Simulated half power beam-width (2x).

Radiation pattern cuts according to Ludwig’s III definition, normalized to directivity, are shown in Figure 9. and Figure 10. For brevity, only the results of Port-X are presented, having Port-Y equivalent performance. Patterns show symmetric shape with low cross-polarization levels within a sufficiently large view angle.

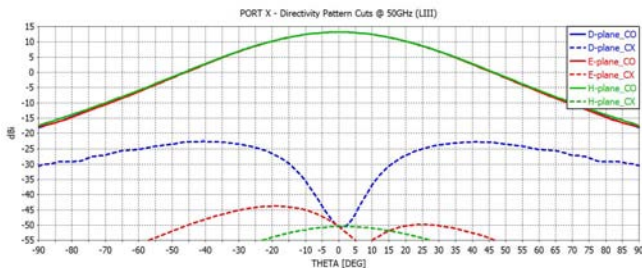


Figure 9. : Simulated directivity pattern cuts for Port-X @ start frequency (50GHz).

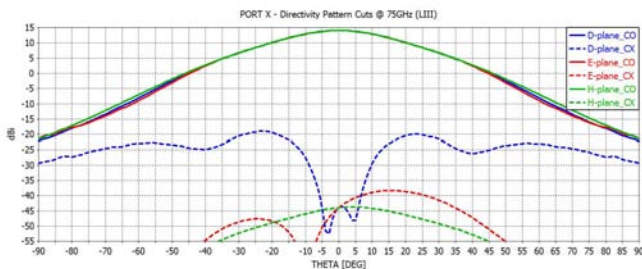


Figure 10. : Simulated directivity pattern cuts for Port-X @ stop frequency (75GHz).

V. PROBE CHARACTERIZATION

The V-band probe design has been manufactured assigning to the hardware model the part number SP50000. A batch of six units was produced and the first unit is shown in Figure 11.



Figure 11. : MVG SP50000 probe (w/o absorber screen).

Initially, the six units have been tested for reflection coefficients to evaluate design repeatability. Then one unit was randomly picked for more detailed testing. All verification testing was performed connecting waveguide-coax adapters [1] to the probe WR-15 input ports. An extract of the interface control drawing showing the port definition and the RF-axes is shown in Figure 12. The upper port, closer to the radiating aperture, feeds the linear polarization aligned with the Y-axis, vice-versa the lower port feeds the X-axis.

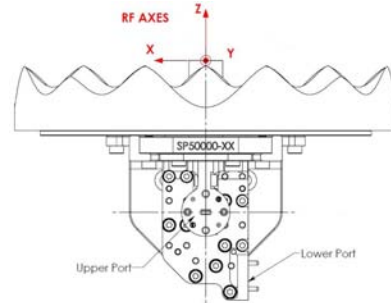


Figure 12. : Interface control drawing, port definition and XYZ reference system.

The set-up for S-parameter measurement is shown in Figure 13. The reflection coefficients have been performed with an Agilent N5242A Vector Network Analyzer with V-band frequency extension module [20] that up converts the system to 50-75 GHz. The test port is calibrated with Agilent 1 mm calibration kit 85059A. The port-to-port isolation was tested with two Tx-Rx frequency extension modules.



Figure 13. : Test set-up for S-parameters: reflection coefficients (left), port-to-port isolation (right).

The input reflection coefficients referenced to 50 Ohms of the six units are shown in Figure 14. Satisfactory matching levels below -10dB have been achieved across the band, even though the contribution of the waveguide-coax adapters (approx. 15dB return loss) was not removed / calibrated out from the test data. Performance repeatability was experienced within the batch, demonstrating a reasonable stability of the manufacturing process.

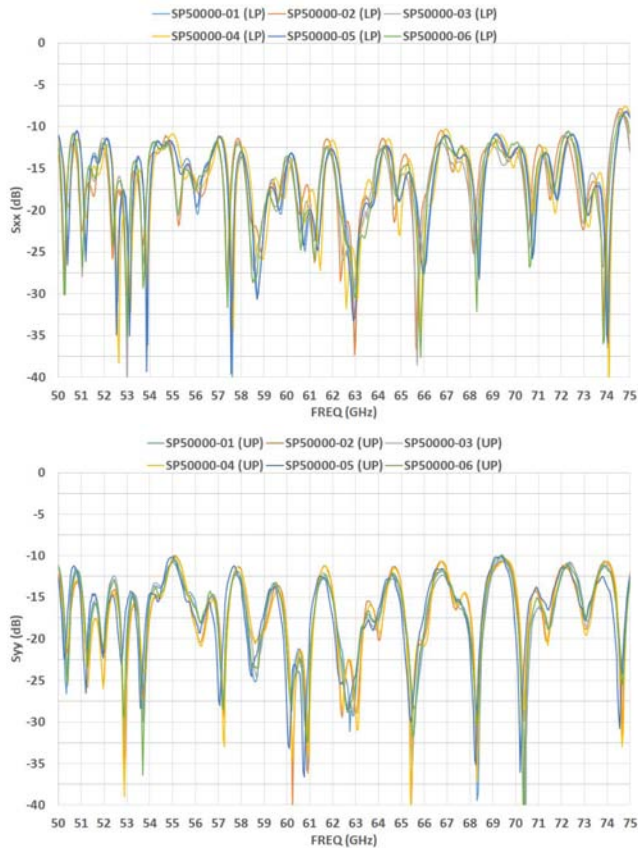


Figure 14. : Measured reflection coefficients referenced to 50 Ohms: probe lower port (top) and upper port (bottom).

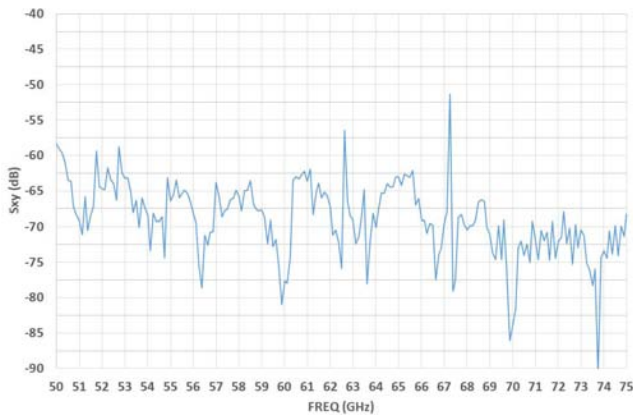


Figure 15. : Measured port-to-port isolation.

After reflection coefficients, the test set-up was modified and the port-to-port coupling of the unit identified by serial number 06 was tested. Figure 15. shows the performance over frequency. The average isolation between ports is excellent, with an average value below 60dB, showing a good manufacturing accuracy and electrical symmetry of the balanced feeding. A few resonant frequencies are visible in the frequency response. Even if this effect is of second order importance, it is being further investigated, mostly in regards of the quality of the ohmic contacts between the probe components. It should be pointed out that this phenomenon is not unusual in nearly loss-free electrically long devices, with RF junctions / discontinuities within the sections.

The randomly picked unit was then tested in MVG μ -Lab system for radiation pattern characteristics. The probe mounted on its test fixture and located in the QZ of the facility is shown in Figure 16.

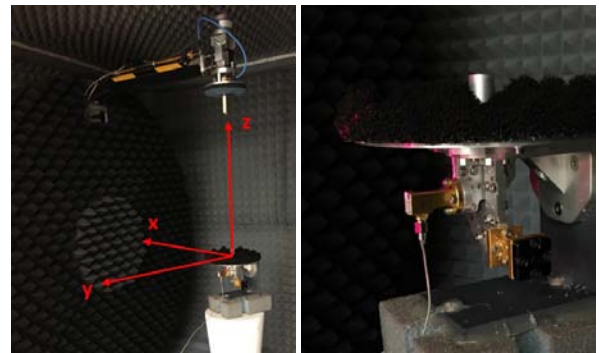


Figure 16. : AUT mounted on the test fixture and XYZ reference system.

The measured boresight directivity and the half power beam-width (2x) are reported in Figure 17. and Figure 18. For boresight directivity levels, the simulated values have been overlaid to the experimental data, showing an excellent agreement. The maximum deviation is 0.1dB worst case. It should be noted that the tested configuration differs from the modeling by the absorbing provisions, which have been replaced by a metallic skirt in the computations. The beam-width data also correlates very well to the simulated data of Figure 7.

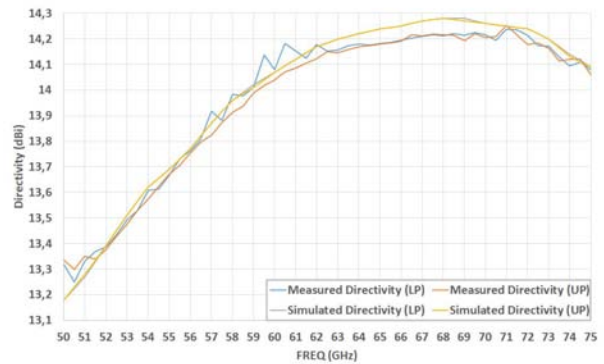


Figure 17. : Boresight directivity: measured versus simulated.

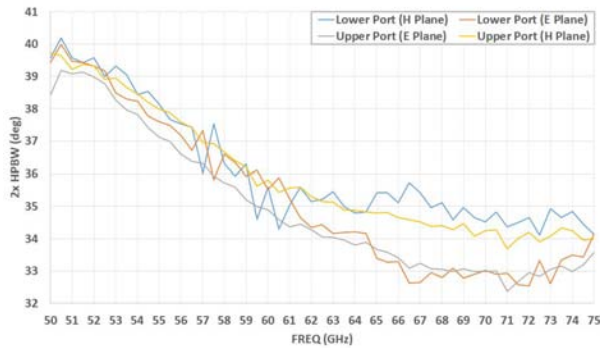


Figure 18. : Measured half power beam-width (2x).

A pattern comparison between experimental and simulated data has been carried out at the test frequency of 60GHz. A spherical wave low pass filtering with modes equivalent to >99.9 power percentage was applied in the NF-FF transformation [21]. Figure 19. shows the lower port pattern cuts in the principal planes, while Figure 20. the comparison for upper port. Simulated cross-polarization data is below the dynamic range of the plot scaling and therefore does not appear in the graphs.

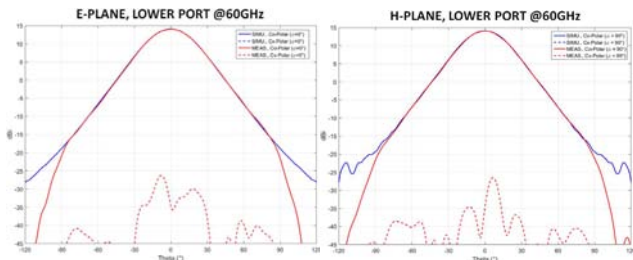


Figure 19. : Lower port, E-plane (left) and H-plane (right).

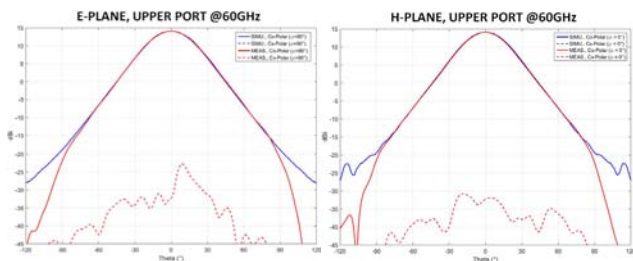


Figure 20. : Upper port, E-plane (left) and H-plane (right).

VI. CONCLUSIONS

MVG has developed a 50 to 75 GHz high performance SNF probe that has been optimized for the MVG- μ LAB systems. Measured data has been presented that shows design requirements were met or exceeded. The agreement between simulation and measured data indicates successful design and manufacturing. Manufacturing six low rate initial production (LRIP) units that all have very closely matching measured data indicates that the fabrication techniques are adequate, reliable and repeatable. The physical and RF performance characteristics of the probe also suggest alternate applications beyond MVG-

μ LAB systems. MVG is also confident that both the fabrication process as well as design features are scalable and will allow future development of probes in band above V-band. The parallel dual receiver design is complete and in production now. The reduction in measurement time is a given based on single sphere measurements. Final implementation will require correction of amplitude and phase imbalances in both the probe and the entire dual receiver paths. This data collection technique, correction coefficient extraction algorithm, and coefficient application software have already been developed, vetted, and implemented by MVG for many years and applied to the MVG SG and StarLab product lines.

REFERENCES

- [1] E. Lee, E. Szpindor, J. Aubin, R. Soerens, "Millimeter Wave Polarization Calibration for Near-Field Measurements", AMTA 2013, Oct. 6-11, Columbus, OH;
- [2] E. Lee, E. Szpindor, W. McKinzie III, "Mitigating Effects of Interference in On-Chip Antenna Measurements", AMTA 2015, Oct. 11-16, Long Beach, CA;
- [3] E. Lee, R. Soerens, E. Szpindor, P. O. Iversen, "Challenges of 60 GHz On-Chip Antenna Measurements", IEEE Antennas and Propagation Society International Symposium, Jul. 19-24, 2015, Vancouver, BC, Canada;
- [4] W. McKinzie III, P. O. Iversen, E. Szpindor, M. Smith, B. Thrasher, "60GHz Reference Chip Antenna for Gain Verification of Test Chambers", AMTA 2016, Oct. 30-Nov. 4, Austin, TX;
- [5] E. Szpindor, W. Zhang, P. O. Iversen, "Measurement Uncertainties in Millimeter Wave On-Chip Antenna Measurements", AMTA 2016, Oct. 30-Nov. 4, Austin, TX;
- [6] http://www.mvg-world.com/en/system/files/-Lab_datasheet_final-EN-jan2015.pdf
- [7] ANSI/IEEE Std 149-1979 "IEEE Standard Test Procedures for Antennas";
- [8] IEEE Std P1720™/D2 (Draft) "Recommended Practice for Near-Field Antenna Measurements";
- [9] L. J. Foged, "Probe Performance Considerations in High-Accuracy Near-Field Measurements", AMTA Event, Boston, July, 21st 2014;
- [10] L. J. Foged, A. Giacomini, H. Garcia, S. Navasackd, C. Bouvin, L. Duchesne, "Wide-band dual polarized probe for accurate and time efficient satellite EIRP/IPFD measurements" AMTA 2005, Oct. 30-Nov. 4, Newport, RI;
- [11] L. J. Foged, A. Giacomini, R. Morbidini, "Probe performance limitation due to excitation errors in external beam forming network", AMTA 2011, October 16-21, Englewood, CO;
- [12] F. Saccardi, A. Giacomini, L. J. Foged, "Probe Correction Technique of Arbitrary Order for High Accuracy Spherical Near Field Antenna Measurements", AMTA 2016, Oct. 30-Nov. 4, Austin, TX;
- [13] L. J. Foged, L. Duchesne, L. Roux, Ph. Garreau, "Wide-band dual polarized probes for high precision near-field measurements", AMTA 2002, 3-8 Nov, Cleveland, OH;
- [14] L.J. Foged, A. Giacomini, R. Morbidini, "Dual-Polarized corrugated horns for advanced measurement applications", Antennas & Propagation Magazine, Vol 52, No 6, December 2010;
- [15] J. Uher, J. Bornemann, U. Rosenberg "Waveguide Components for Antenna Feed Systems: Theory and CAD", Artech House, Chapter 3;
- [16] A. M. Bøifot "Classification of Ortho-Mode Transducers", European Trans. Telecommunications and Related Technologies, vol. 2, no. 5, pp. 503-510, Sept. 1991;
- [17] www.cst.com, CST STUDIO SUITE™, CST AG, Germany;
- [18] [https://en.wikipedia.org/wiki/Waveguide_\(electromagnetism\)](https://en.wikipedia.org/wiki/Waveguide_(electromagnetism))
- [19] <http://www.sagemillimeter.com/>
- [20] <https://www.vadiodes.com/en/>
- [21] http://www.mvg-world.com/en/system/files/SOFT_MV-Echo_2014_bd.pdf